Journal of Chromatography A 1718 (2024) 464721

Contents lists available at ScienceDirect

Journal of Chromatography A

journal homepage: www.elsevier.com/locate/chroma

Application of Raman spectroscopy during pharmaceutical process development for determination of critical quality attributes in Protein A chromatography

Jingyi Chen [a,b], Jiarui Wang [a], Rudger Hess [a], Gang Wang [a], Joey Studts [a], Matthias Franzreb [b,*]

[a] Boehringer Ingelheim Pharma GmbH / Co. KG, Biberach an der Riss, Germany
[b] Institute of Functional Interfaces, Karlsruhe Institute of Technology, Eggenstein-Leopoldshafen 76344, Germany

ARTICLE INFO

Keywords:
Therapeutic antibody
Process analytical technology
Process robustness
Machine learning
In-line monitoring

ABSTRACT

Raman spectroscopy is considered a Process Analytical Technology (PAT) tool in biopharmaceutical downstream processes. In the past decade, researchers have shown Raman spectroscopy's feasibility in determining Critical Quality Attributes (CQAs) in bioprocessing. This study verifies the feasibility of implementing a Raman-based PAT tool in Protein A chromatography as a CQA monitoring technique, for the purpose of accelerating process development and achieving real-time release in manufacturing. A system connecting Raman to a Tecan liquid handling station enables high-throughput model calibration. One calibration experiment collects Raman spectra of 183 samples with 8 CQAs within 25 h. After applying Butterworth high-pass filters and *k*-nearest neighbor (KNN) regression for model training, the model showed high predictive accuracy for fragments (Q^2 = 0.965) and strong predictability for target protein concentration, aggregates, as well as charge variants ($Q^2 \geq$ 0.922). The model's robustness was confirmed by varying the elution pH, load density, and residence time using 19 external validation preparative Protein A chromatography runs. The model can deliver elution profiles of multiple CQAs within a set point ± 0.3 pH range. The CQA readouts were presented as continuous chromatograms with a resolution of every 28 s for enhanced process understanding. In external validation datasets, the model maintained strong predictability especially for target protein concentration ($Q^2 = 0.956$) and basic charge variants ($Q^2 = 0.943$), except for overpredicted HCP ($Q^2 = 0.539$). This study demonstrates a rapid, effective method for implementing Raman spectroscopy for in-line CQA monitoring in process development and biomanufacturing, eliminating the need for labor-intensive sample pooling and handling.

1. Introduction

In the biopharmaceutical industry, it is increasingly challenging to enhance the productivity of research and development (R&D), facilitate efficient regulatory compliance, and shorten timeline from drug discovery to market [1,2]. Over the past decade, enhancement in productivity and efficiency of upstream and downstream processing was driven by innovation in technology [3], as process intensification [4] and continuous manufacturing [2,5,6] evolve to be key trends in biomanufacturing. Mechanistic modeling has also been widely investigated and implemented in downstream processes for deep physical understanding and process knowledge [7]. In 2004, the US Food and Drug Administration (FDA) [8] encouraged the use of Process Analytical Technology (PAT) to ensure consistent product safety, quality, and efficacy with enhanced process understanding. In line with ICH Q13 guideline [5], PAT enables the measurement of drug substances and impurities during continuous manufacturing to facilitate real-time monitoring of manufacturing processes and process control [6,9]. The industrial bioprocess development is striving to meet the quality by design (QbD) [10] paradigm to achieve a greater understanding of critical quality attributes (CQAs) [2,11]. PAT is considered a complementary technology for facilitating biomanufacturing through diverse analytical techniques and chemometric models [12,13]. Within the frame of PAT, in-line CQA monitoring is often desired in downstream process (DSP) for the purpose of accelerating process development and achieving real-time release in manufacturing.

In the past few years, researchers have been testing a series of analytical techniques as PAT tools. Rolinger and coworkers [14]

* Corresponding author.
E-mail address: matthias.franzreb@kit.edu (M. Franzreb).

https://doi.org/10.1016/j.chroma.2024.464721
Received 14 November 2023; Received in revised form 5 February 2024; Accepted 6 February 2024
Available online 8 February 2024

compared UV and Raman spectroscopy in monitoring the protein concentration during Protein A chromatography using Partial Least Square (PLS) models and Convolutional Neural Networks (CNN), showing improved predictability with the UV-based model. Infrared spectroscopy was investigated for in-line protein concentration measurements in ion-exchanged chromatography by Akhgar et al. [15]. Patel and coworkers [16] made progress on using a multi-angle light scattering system as PAT tool in real-time molecular weight measurements in hydrophobic interaction chromatography. Furthermore, water proton nuclear magnetic resonance spectroscopy under flow conditions (flow-wNMR) was proposed as a PAT tool for protein concentration and aggregates by Taraban and coworkers [17]. Based on the current research on PAT, Raman spectroscopy is considered a high-potential technique for in-line CQA measurements in downstream processes [6, 14]. Initial progress made on Raman application in chromatography was presented by Feidl and coworkers [12] in 2019, comprising a novel flow cell and chemometric protocol for monitoring protein concentration in chromatography with in-line Raman spectroscopy. Zhang et al. [18] proposed a quantitative determination of aggregates based on Raman spectroscopy. Rolinger et al. [14] employed non-linear models CNN and data fusion in the model regression between Raman spectra and protein concentration, introducing a novel way of generating regression models using machine learning. Wei and coworkers [19] demonstrated the feasibility of a multi-attribute Raman spectroscopy (MARS) in drug substance development, the first study to quantify multiple product quality attributes (PQAs) with a single method.

Our previous work demonstrated that automated calibration and in-line Raman detection [20] contribute to a dramatic reduction in intensive lab-work and material requirements, allowing for the efficient establishment of machine learning models. High-throughput Raman collection was achieved by connecting Raman to a Tecan Liquid Handling robot, leading to success in accurately determining in-line aggregates and fragments during the Protein A chromatography elution phase [21]. In this study, a KNN regression following a series of Butterworth filters was applied to generate Raman-based model for CQA predictions in Protein A chromatography. The time-consuming measurement and evaluation of various analytical techniques are considered a bottleneck for biopharmaceutical process development. The Raman model is an alternative for in-line monitoring in DSP, measuring CQAs without having pool analytics. But for successful implementation, feasibility assessment of the Raman model should be performed on actual DSP scenarios, including internal and external model validation to test the robustness and interpolation ability of the Raman-based model.

In the field of biopharmaceutical development and manufacturing, various PAT tools have been implemented and verified. For example, Williams et al. [22] introduced a refractometry-based PAT system to monitor the cell culture metabolic activity with pH control strategy in a lentiviral vector (LVV) production bioprocess. São Pedro et al. [23] implemented a fluorescent dye (FD)-based microfluidic biosensor for real-time aggregation detection in an integrated lab-scale downstream process. Regarding the application of Raman spectroscopy in ultra- and diafiltration processes, Rolinger and coworkers [24] showcased its potential for in-line protein concentration and buffer exchange monitoring. Compared to the predecessors' work, we are the first to develop a Raman-based PAT tool that expended the technical ability of using Raman spectroscopy for measuring and predicting fragments, charge variants, and host cell proteins. The ability has been included into the settings of the process robustness study and, hence, into the monoclonal antibody (mAb) process development. The aim of the study is to develop a Raman spectroscopic method for the determination of CQAs and to verify this method's predictability with 19 Protein A chromatography processes performed within a broad range of process parameters. The purpose of these 19 Design of Experiments (DoE) runs is to investigate the process robustness. To collect Raman datasets for training and internal validation, we performed a fractional Protein A chromatography run followed by a high-throughput calibration experiment and off-line analytics. Subsequently, using a series of Butterworth filters and the KNN regression, we developed a Raman-based predictive model for the determination of concentrations of the target proteins, high and low molecular weight species (HMW & LMW), acid and basic peak groups (APG & BPG), and host cell proteins (HCP). For those species, the model's predictability based on the in-line Raman spectra of the 19 Protein A chromatography runs was challenged by comparing the model outputs with the corresponding off-line measurements. This investigation validated the Raman-based predictive model for in-line determination of CQAs in Protein A chromatography and marks the latest development milestone of Raman spectroscopy application in the field of biopharmaceutical process development.

2. Materials and methods

2.1. Robustness study of a Protein A chromatography

During downstream process development, a robustness study of Protein A chromatography step was conducted for an IgG1 antibody, mAb (Boehringer Ingelheim Pharma GmbH & Co. KG, Biberach, Germany). In the study, the mAb feedstock was harvest cell culture fluid (HCCF) with a titer of 6.42 g/L. MabSelect PrismA (Cytiva, Uppsala, Sweden) resin was used for Protein A chromatography. A column with a diameter of 1 cm and a height of 20.6 cm (i.e., CV = 16.18 mL) was packed for the robustness study. As listed in Table 1, 19 DoE runs were designed and varied with three process parameters, including elution pH, load density, and residence time. All the Protein A chromatography runs were carried out with a pH step elution, on an ÄKTA avant 25 system (Cytiva, Uppsala, Sweden) under control of UNICORN™ 7.5 software. For in-line Raman detection, a Raman flow cell with a dead volume 240 µL (Marqmetrix, Seattle, Washington, USA) was integrated into the ÄKTA system in between the conductivity and pH sensors. This flow cell was connected to a HyperFlux Pro Plus Raman spectrometer (Tornado Spectral Systems, Mississauga, Ontario, Canada) equipped with a 785 nm emission laser. During all DoE runs, the Raman acquisition setup was set to a laser power of 350 mW with a 350 ms exposure time averaged over 20 exposures per scan (measuring time 7 s per spectrum) to avoid saturated detection. An ÄKTA I/O box was installed

Table 1
Overview of DoE input parameters and pool concentrations in project framework for the purpose of investigating process robustness.

Exp. no.	Input parameters			Output
	Load density	Elution pH	Residence time	Pool concentration [g/L]
1	0	0	0	21.71
2	−1	0	0	16.80
3	1	−1	−1	27.63
4	−1	0	1	16.90
5	0	1	0	15.30
6	1	0	0	28.03
7	0	0	−1	21.97
8	0	−1	1	25.83
9	−1	−1	−1	18.68
10	−1	1	−1	11.10
11	1	−1	1	25.92
12	−1	1	1	14.10
13	0	0	0	21.66
14	−1	−1	1	16.23
15	1	1	−1	17.63
16	0	1	1	18.43
17	0	0	0	21.07
18	−1	−1	0	16.93
19	1	1	1	20.15

Three set points are chosen for each single input parameter, labeled as −1, 0, 1. Pool concentrations refer to off-line pool measurements. The experiments numbered by 1, 13, 17 are replicates in the designed experiments.

and used for time synchronization of Raman detection with the chromatography unit. Elution pooling was triggered once the UV absorbance at 280 nm reached 200 mAU, and subsequently stopped when the UV absorbance dropped below 200 mAU. After measuring the protein concentration, the elution pool was frozen at −70 °C. Once all 19 DoE runs were conducted, the pools were thawed at 25 °C and measured by various analytical techniques for CQA determination. The in-line measured Raman spectra of the elution phase were averaged every 4 spectra to reduce the signal-to-noise ratio, obtaining a dataset with a 28 s resolution. The 19 datasets were used for external validation of Raman model trained.

2.2. Fractional Protein A chromatography for internal validation

For internal validation, one fractional Protein A chromatography step was conducted using the same HCCF materials, but one column with a 2.6 cm diameter and a height of 10.5 cm (i.e., CV = 55.75 mL). The experiment was performed on the same ÄKTA system, using an identical in-line Raman detection configuration as employed in the robustness study. The more detailed information about the process and setup has been explained by Wang et al. [21]. Fraction collection was triggered once the UV absorbance at 280 nm reached 200 mAU, and subsequently stopped when the UV absorbance dropped below 200 mAU. The eluant was collected in 25 fractions with a volume of 6 mL each. The pre-eluate was also collected as a single fraction, thus in total 26 fractions. As in the robustness study, the averaged in-line Raman spectra (28 s resolution) of the elution phase were used as an internal validation dataset for model performance evaluation.

2.3. Off-line Raman detection for model training

The 26 fractions obtained from the fractional Protein A chromatography step were followed by a blank sample with elution buffer, in total 27 samples. Using a Tecan Fluent 1080 Liquid Handler (Tecan, Männedorf, Switzerland), each two in sequence of the 27 samples with known quality attributes were automatically mixed with 6 different fractional ratios, resulting in 156 expanded data points of the elution profile. This procedure ultimately yielded a total of 183 samples with mathematically derived quality attributes. Subsequently, the 183 fractions were automatically injected into a Raman flow cell connected to the Tecan system. The flow path was cleaned with 1 M NaOH, 1 M acetic acid, and purified water after every sample measurement. A Raman spectrometer located near the Tecan system was turned on for 25 h, continuously collecting Raman spectra of the samples. The off-line collected and sorted Raman spectra were averaged every 4 spectra and used as a training dataset.

2.4. Off-line analytical reference methods

Four analytical assays were performed for CQA determination of the 25 elution fractions. A NanoDrop One UV–vis Spectrophotometer (Thermo Fisher Scientific, Madison, WI, USA) was used for protein concentration measurement. Size exclusion chromatography (SEC) was performed on a Waters Acquity Ultra Performance LC (Waters Cooperation, Milford, MA, USA) for the determination of aggregates, fragments, and the SEC main peak. High-performance strong cation exchange chromatography (HP-SCX) was intended for APG, BPG, and the SCX main peak, conducted on a Waters system. HCP quantification was carried out on an Octet HTX system (Fortebio, Fremont, CA, USA) using an Octet Anti-CHO HCP Kit (Sartorius AG, Goettingen, Germany).

2.5. Model training, internal and external validation

Raw Raman spectra consist of intensities at 3101 wavenumbers, ranging from 200 to 3300 cm^{-1}. To eliminate flow rate and instrument effects, we preprocessed all the averaged Raman spectra by using a series of Butterworth high-pass filters. Those filters were determined by 155 different cutoff frequency coefficients, which were calculated using a geometric sequence ($2^{-2.5}$, $2^{3.0}$) over a given cutoff value range (−2.5, 3.0). Subsequently, min-max normalization was applied to the filtered spectra due to data scaling, a requirement for *k*-nearest neighbor (KNN) algorithm. Following the preprocessing procedure, Raman spectra of 183 samples were transformed into a 2-dimensional Raman image matrix with dimensions (183, 155, 3101). A KNN regressor with 32 neighbors ($k = 32$) was then employed to correlate spectral features with the 8 CQAs reference results, thereby developing a Raman-based KNN model. In the model regression algorithm, attributes related to SEC and SCX are multiplied by protein concentration and converted from percentage to g/L. In the KNN regressor, the training dataset was derived from a random sampling of the preprocessed 2-dimensional Raman image matrix, following a Gaussian distribution with standard deviations equivalent to 2-fold dataset errors. This sampling process was repeated ten times, yielding a matrix shape of (1830, 155, 3101). Similarly, the analytical label matrix Y, with dimensions (1830, 8), was generated through random sampling from a Gaussian distribution with a standard deviation of 0.01, also conducted ten times.

The upper limit of the cutoff frequency range and the *k*-value are regarded as two determinative hyperparameters to be tuned for model optimization. Hyperparameter screening experiments were performed on the training dataset, followed by internal validation using the in-line Raman dataset from the fractional Protein A chromatography to evaluate model's performance. The evaluation of regression analysis involved metrics such as the coefficient of prediction (Q^2) and the Mean Absolute Percentage Error (MAPE) between off-line measurements and in-line Raman predictions. An initial grid search study was conducted with 12 evenly spaced frequency cutoff values in the range of (1.5, 7) and 13 evenly spaced *k*-values in the range of (8, 104). The outcome indicated that the models operating on cutoff values of 3, 3.5 and 4 have better performance with higher Q^2 and lower MAPE. The subsequent fine-tuning was carried out applying the combination of 11 cutoff values in the range of (3, 4) and 10 *k*-values in the range of (8, 80). The optimal model, featuring a cutoff value of 3.0 and a *k*-value of 32, was determined based on the lowest MAPE and higher Q^2 values.

The trained model's predictability was examined through external validation using datasets from 19 external Protein A chromatography DoE runs. The accuracy of the model in predicting 8 CQAs was assessed by comparing its predictions with pool analytical results as a reference. The average value of each CQA in each DoE run was calculated, considering the duration time from the initiation of pooling to regeneration. These average values served as the in-line pool predictions, and the model's performance was evaluated using the same metrics Q^2 and MAPE, as employed for internal validation. Due to the absence of pool materials for HCP measurements in DoE runs 13, 17, and 19, these three DoE runs were excluded from the HCP performance metrics assessment.

3. Results and discussion

3.1. Model optimization and internal validation

To develop a Raman-based model and test whether the model can in-line predict all the CQAs, we performed two types of Raman detection on the same samples, using off-line dataset for model training and in-line dataset for internal validation. First, we conducted a Protein A chromatography run with in-line Raman detection, collecting 26 elution fractions and their in-line Raman dataset (4 spectra × 26 fractions × 8 CQAs). The fractions of various measured CQAs were followed by a blank sample with elution buffer, in total 27 samples. Each two in sequence of the 27 samples with known quality attributes were mixed with 6 different fractional ratios, resulting in 156 expanded data points of the elution profile. This procedure ultimately yielded a dataset of 183 samples with mathematically derived quality attributes, which was used for the model calibration. Subsequently, the continuous acquisition of

Raman spectra of each of the 183 samples lasted for 5 min. A hardware system connecting Raman to a Tecan Liquid Handling robot assisted in high-throughput mixing and Raman acquisition of the 183 samples within 25 h, obtaining a large off-line Raman dataset (40 spectra × 183 samples × 8 CQAs). Due to different handling of the same elution fractions, it was necessary to apply the same preprocessing methods on both Raman datasets to remove the differences in hardware system and flow rate [21]. Raw Raman spectra consist of intensities at 3101 wavenumbers. We averaged the raw Raman spectra every 4 spectra and preprocessed them using a series of Butterworth high-pass filters, to which 155 different cutoff frequency coefficients were applied. The 155 cutoff frequency coefficients were computed by a geometric sequence ($2^{-2.5}$, $2^{3.0}$) over a given cutoff value range (−2.5, 3.0). Min-max normalization was applied to the filtered spectra. The upper limit of the cutoff frequency range and the *k*-value are regarded as two determinative hyperparameters to be tuned for model optimization. After preprocessing, the Raman-based model was trained on the off-line Raman dataset of the 183 samples, and then internally validated on the in-line Raman dataset of the 26 fractions. Model optimization finds the optimal hyperparameter combination, a cutoff value of 3.0 and a *k*-value of 32, based on the coefficient of prediction (Q^2) and the Mean Absolute Percentage Error (MAPE) of internal validation.

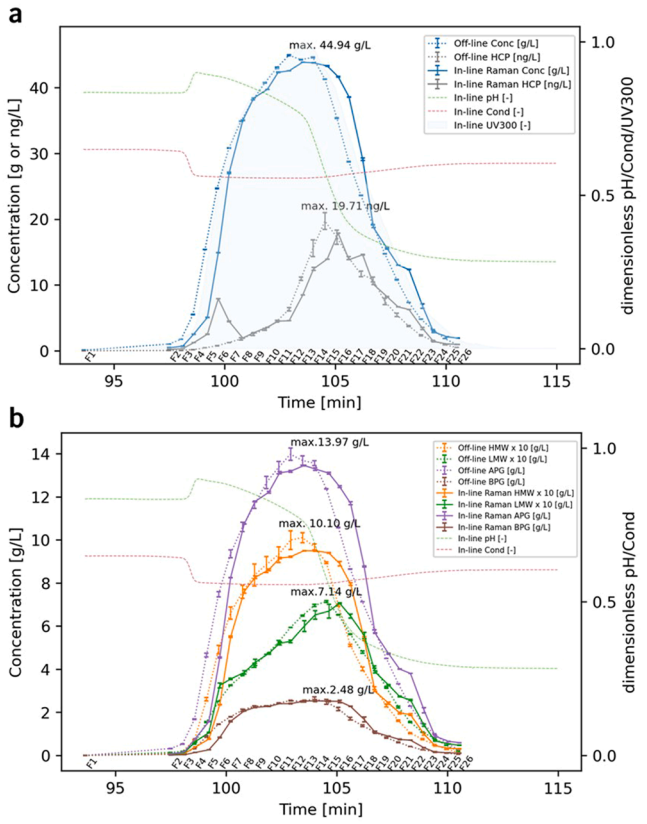

Fig. 1. Comparing off-line measurements and in-line Raman predictions of 26 elution fractions for 6 critical quality attributes (CQAs). F1-F26 refer to the 26 fractions eluted from Protein A chromatography used for model calibration. Off-line and in-line data are compared regarding (a) target protein (Conc) and host cell proteins (HCP), (b) high/low molecular weight (H/LMW) and acid/basic peak group (A/BPG). The primary *Y*-axis indicates CQA concentrations in g/L or ng/L. H/LMW concentrations are multiplied by 10 times for clear illustration. The maximum concentration about each CQA is given in the figures as additional information. In-line UV absorbance at 300 nm (in a light blue elution shape), pH (green dashed line) and conductivity (rose dashed line) values exported from Unicorn software are converted to a dimensionless unit and presented on a secondary *Y*-axis. (For interpretation of the references to color in this figure legend, the reader is referred to the web version of this article.)

Fig. 1 shows the elution chromatograms of the training experiment, comparing the off-line measurements with in-line CQAs predicted by the KNN model. The CQAs of the 26 elution fractions (from F1 to F26) used for model calibration are displayed in concentration on the primary *y*-axis. The concentrations of target proteins and HCP are presented in Fig. 1(a), together with the in-line UV absorbance curve at 300 nm. The off-line and in-line target protein concentration correspond with UV300. Aggregates, fragments, and charge variants are concentration-dependent and exhibit similar tailing concentration profiles to protein concentration, as demonstrated in Fig. 1(b). Fig. 1(b) illustrates the model's robust predictions for fragments, which have a shape closely resembling the off-line profile. The in-line pH curve represents a step-wise pH elution applied to this Protein A chromatography run. Following the pre-elution phase of about 5 min, target proteins and impurities are eluted from the resin with a decrease in pH and conductivity values. A significant decrease in pH and slight increase in conductivity are detected at the time point near maximum protein concentrations. Compared with off-line measurements, significantly higher in-line predictions of target protein (Fig. 1(a)), HMW, APG, and BPG (Fig. 1(b)) are observed starting from the sharp pH turning point in fraction 14 (F14). However, the model predictions for LMW (Fig. 1(b)) and HCP (Fig. 1(a)) appear to be less impacted by the same changes in pH. From fractions 3 to 8 (F3 to F8), the trained model has significantly lower predictions for target protein, HMW, APG, and BPG compared to off-line measurements. Furthermore, an unexpected prediction peak between fractions 3 and 8 is noticed.

The correlations between off-line measurements of 26 fractions and in-line predictions were illustrated in Fig. 2 for 8 CQAs. In the internal validation dataset, the model demonstrates robust predictive performance for fragments, where the in-line predictions have a shape closely resembling the off-line profile ($Q^2 = 0.965$) and a minimal MAPE value of 22.13 % (Figs. 1(b), 2(c)). For protein concentration (Fig. 2(a)), aggregates (Fig. 2(b)), charge variants (Fig. 2(d), (e)) and main peak of SEC and SCX (Fig. 2(g), (h)), the calibration model has strong predictability, reaching a Q^2 of at least 0.922. However, when examined closely, the correlations for those CQAs show a weaker linearity within the medium concentration range. These discrepancies in the correlations are in agreement with the significantly higher predictions observed from F14 and lower predictions from F3 to F8. The deviations in the predictions can be attributed to changing process conditions, particularly the alterations in pH. During the model calibration, the KNN regressor demonstrated a limited capability in extracting the spectral features related to pH. Regarding the HCP, the unexpected prediction peak between F3 and F8 results in a MAPE value of 142.91 % (Figs. 1(a), 2(f)). The model is therefore less predictive in terms of HCP than the other CQAs.

Based on the internal validation results, the trained Raman model has robust predictability for protein concentration, aggregates, fragments, charge variants, and main peak of SEC and SCX. However, the model's prediction accuracy may be affected by fluctuations in elution pH. Moreover, the model's predictive performance for HCP is unsatisfactory. Overall, the internal validation results demonstrate that the trained calibration model can predict 8 CQAs simultaneously.

3.2. *Raman predictions on a process robustness study for external model validation*

During the process development, a robustness study was performed on the Protein A chromatography step to test acceptable ranges of three process parameters, including elution pH, load density, and residence time. Three varied set points were selected for each parameter, as listed in Table 1, resulting in a total of 19 DoE runs. In the study, in-line Raman detection was applied to the 19 runs to verify the trained Raman model's predictability in CQA determination. The resulting in-line Raman data were used for external validation of the trained model. To evaluate the

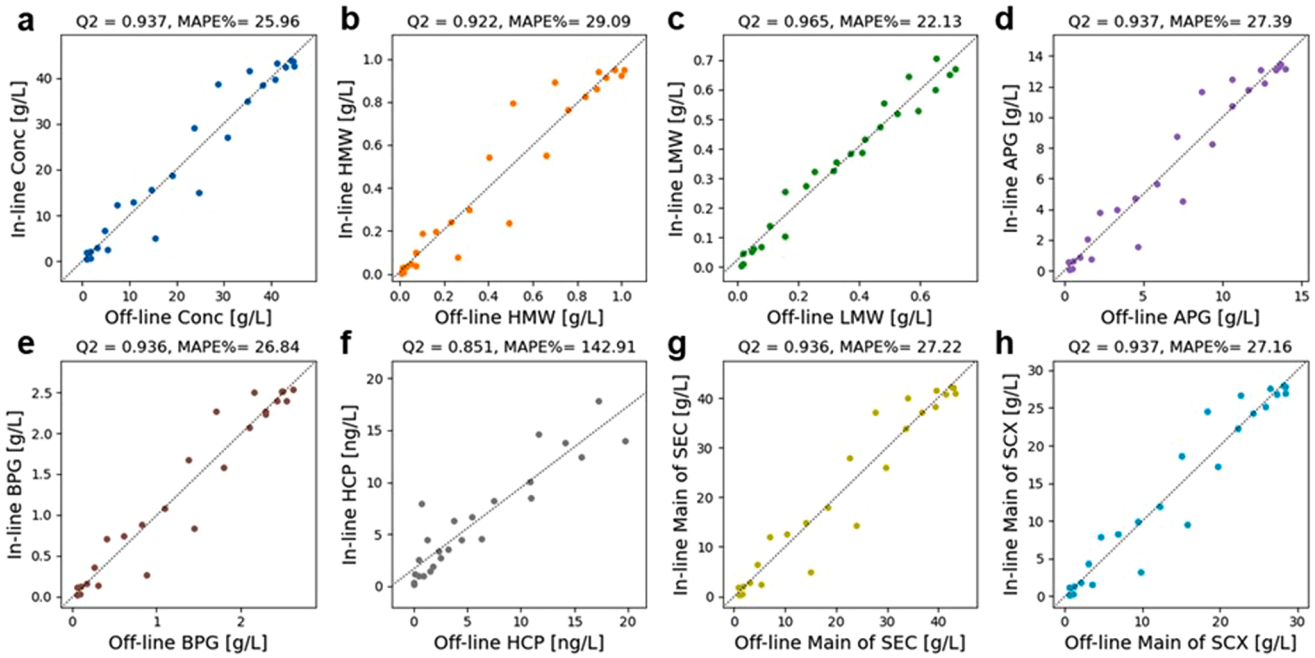

Fig. 2. Comparison of off-line fractional measurements and in-line predictions applied the trained Raman model for 8 critical quality attributes. The corresponding metrics Q2 and MAPE in percent were displayed in the regression plots for (a) protein concentration, (b) high molecular weight (HMW) or aggregates, (c) low molecular weight (LMW) or fragments, (d) acid charge variants APG, (e) basic charge variants BPG, (f) host cell proteins (HCP), the main peak of (g) size variants SEC and (h) charge variants SCX.

model performance on the DoE runs, we calculated the pool concentration of CQAs according to in-line Raman predictions and compared it with off-line pool analytical results. Model performance on external validation datasets is interpreted by metrics Q^2 and MAPE. Table 2 summarizes all the performance metrics of the trained Raman model in terms of 8 CQAs. Additionally, one-way Analysis of variance (ANOVA) test was employed to provide statistical evidence of whether the varied process parameters have a significant impact on the model prediction accuracy of 8 CQAs. The test compares the means of the four categorical groups, which refers to the three process parameter inputs and deviations between predictions and observations regarding one of the 8 CQAs. Table 3 presents the ANOVA test's results for the process parameters for the 8 CQAs, taking the significance level of 0.05 as the threshold. The DoE runs 3, 6, 8, and 11 were not taken into account in the ANOVA test. The elution profiles of these DoE runs were saturated, as the predicted concentration exceeds the dynamic range of the trained model. The dynamic range of a calibration model can be regarded as the broadest concentration range that the model calibrates. Within this dynamic range, the model can determine the concentration quantitatively with certain accuracy and precision. For instance, the target protein concentration in the model calibration ranges from a minimum of 0 g/L to a maximum of 44.94 g/L, as represented in Fig. 1. A p-value of 0.002 between elution pH and the deviation in aggregates indicates that the aggregate prediction error has significant correlation with elution pH. Furthermore, the two process parameters, load density and residence time, have no significant impact on the prediction accuracy of the trained Raman model with respect to the 8 CQAs ($p > 0.05$).

Fig. 3 presents the elution profiles of target proteins and impurities for the 19 DoE runs. These profiles are predicted by the trained Raman model. The in-line pH and conductivity curves indicate the process parameter variances of these 19 DoE runs, and the differences in the shape of UV300 reflect the variances in process performance. To assess the Raman model's ability to identify proteins or buffer in the eluates, the starting elution, pooling and regeneration time points are matched to each DoE run and marked in the subfigures. The Raman model only identifies process buffer without proteins during the pre-elution phase in all runs. The predicted elution profiles of CQAs first arise until the corresponding starting pooling time. Obviously, the elution profiles of in-line concentration predictions match with the UV300 shapes, except

Table 2
Performance metrics of the regression model in terms of 8 critical quality attributes.

Critical quality attributes (CQAs)	Model performance metrics			
	internal validation		external validation	
	Q^2	MAPE (%)	Q^2	MAPE (%)
Concentration	0.937	25.96	0.956	3.67
High molecular weight (HMW)	0.922	29.09	0.567	33.40
Low molecular weight (LMW)	0.965	22.13	0.734	12.59
Acid peak group (APG)	0.937	27.39	0.814	9.62
Basic peak group (BPG)	0.936	26.84	0.943	6.41
Host cell proteins (HCP)	0.851	142.91	0.539	259.93
Main peak of size variants (SEC)	0.936	27.22	0.950	4.01
Main peak of charge variants (SCX)	0.937	27.16	0.960	4.29

The model's accuracy and predictability on each CQA were evaluated on both internal and external validation datasets, using the coefficient of prediction (Q^2) and the Mean Absolute Percentage Error (MAPE).

Table 3
Analysis of variance (ANOVA) test's p-values for three process parameter inputs in terms of 8 CQAs.

Deviation in CQAs (Critical quality attributes)	p-value of ANOVA analysis		
	Elution pH	Load density	Residence time
Concentration	0.178	0.407	0.252
High molecular weight (HMW)	0.002	0.621	0.363
Low molecular weight (LMW)	0.483	0.081	0.464
Acid peak group (APG)	0.222	0.381	0.754
Basic peak group (BPG)	0.224	0.970	0.516
Host cell proteins (HCP)	0.452	0.809	0.479
Main peak of size variants (SEC)	0.531	0.600	0.241
Main peak of charge variants (SCX)	0.382	0.902	0.441

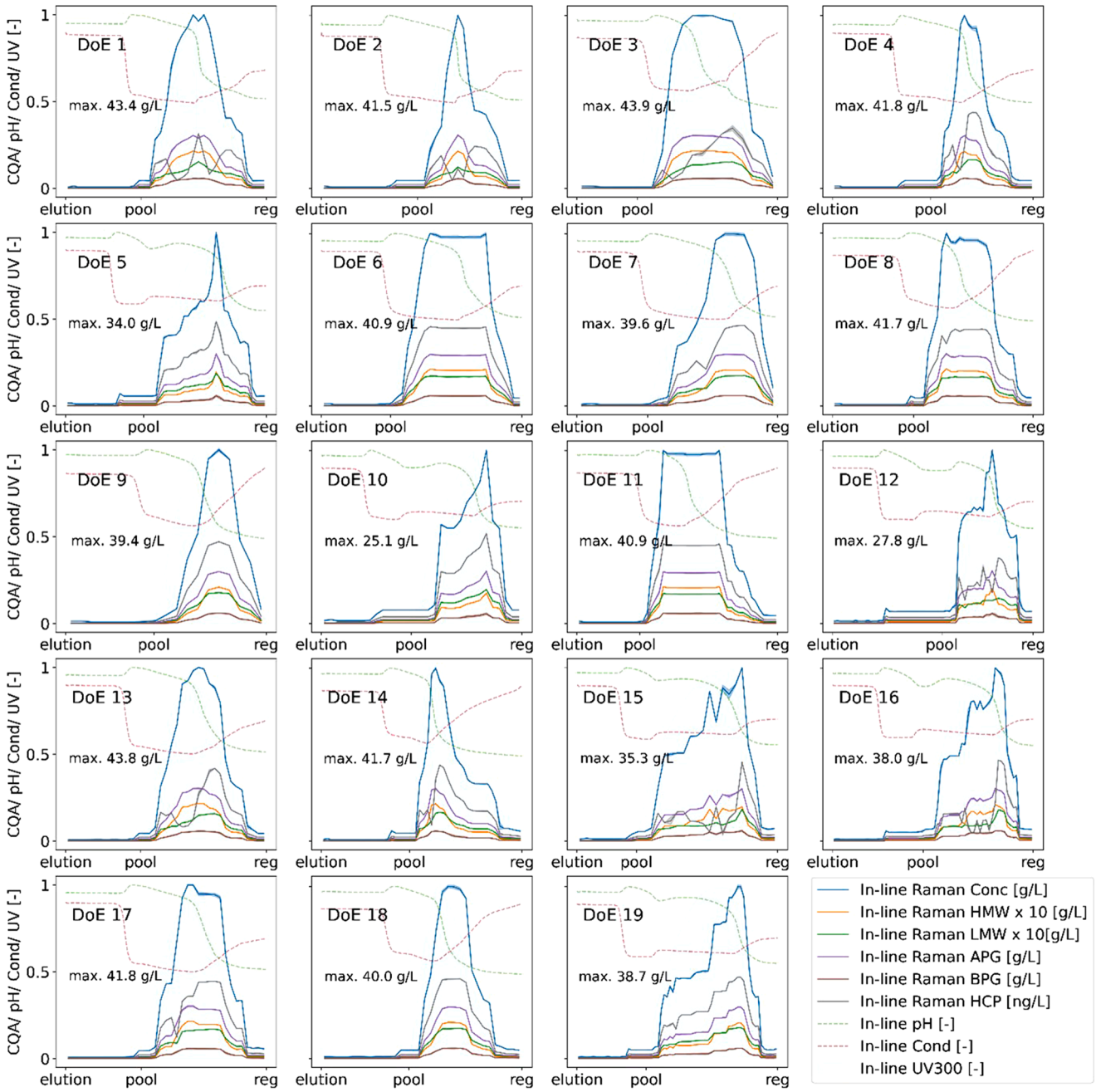

Fig. 3. A single Raman-based model predicting in-line concentrations of multiple critical quality attributes (CQAs) in continuous chromatograms at 28-second intervals. The elution chromatograms of 19 Design of Experiments (DoE) runs are predicted by the trained Raman model, for the concentrations of target proteins, high/low molecular weight (H/LMW), acid/basic peak group (A/BPG) and host cell proteins (HCP). All the represented CQA concentrations are normalized along the *Y*-axis, ranging from 0 to 1, by dividing all Raman predictions by the maximum predicted target protein concentration, along with corresponding 95 % confidence interval. The maximum predicted target protein concentration was displayed in every DoE plot. In-line pH, conductivity and UV absorption at 300 nm (UV300) are converted to a dimensionless unit. The offset of conductivity is manually adjusted and zoomed in for the purpose of a clear overview. For every DoE, the initiation of elution, pooling, and regeneration time points are synchronized with the corresponding data obtained from the Unicorn software.

for DoE runs 3, 6, 8, and 11. In these DoE runs, the predicted elution profiles appear to be saturated and limited by the model's dynamic range. Although the measured UV300 curves are not saturated. These saturated elution profiles are a consequence of the actual protein concentrations exceeding the model's dynamic range. A stepped and discrete shape of concentration profiles is noticeable across the DoE runs 5, 10, 12, 15, 16, and 19 in Fig. 3. In contrast to other runs, the pH or conductivity profiles in these six DoE runs are noticeably arched or concaved before the starting pooling points. This common feature arises from the high elution pH level (set point +0.3), as listed in Table 1. Consequently, these six DoE runs highlight a limitation of the current trained Raman model at the pH condition of set point +0.3. DoE runs 1, 13, and 17 act as three replicate DoE runs. Except for HCP, identical concentration profile shapes are achieved in DoE runs 1 and 13. However, the predicted target protein concentration in the tailing part of the elution profile of DoE run 17 deviates from the UV300 signal.

When the model is applied to a process robustness study in downstream process development, it is demonstrated that a single Raman-based model can deliver a full picture of target proteins and impurities, without the need for lab-intensive fractionation and industry

standard pool analytics. In the 19 external validation DoE runs, the Raman model demonstrates its ability to differentiate the process buffer and proteins. Regarding target protein concentration, APG, BPG, and main peak of SEC and SCX, the model shows strong predictability with good accuracy. The model can also provide with a high resolution of every 28 s, enabling continuous chromatograms of target proteins and impurities in DSP development and manufacturing. However, it is important to note that the model's performance can be significantly affected by fluctuations in pH condition, leading to inaccurate elution profile shapes of protein concentrations. The influence of pH ranges should be comprehensively included in the model calibration and training by using additional samples with varied pH or by an interlinked advanced model regression approach. Additionally, the model's precision in predicting the HCP profile is not as precise as desired. Dedicated fractional samples would allow a deeper evaluation of the model's precision for other CQAs.

Off-line measurements and in-line predictions of the 19 pool samples, along with performance metrics for the 8 CQAs are displayed in relation to elution pH-value in Fig. 4. Towards protein concentration (Fig. 4(a)), the Raman model fits the observations well, with a slight deviation at high concentration observed, obtaining a Q^2 of 0.956 and a MAPE of 3.67 %. Within an elution pH range of set point ± 0.3, the model has strong predictability on APG ($Q^2 = 0.814$ with MAPE = 9.62 %, in Fig. 4(d)), BPG ($Q^2 = 0.943$ with MAPE = 6.41 %, in Fig. 4(e)), the main peak of SEC ($Q^2 = 0.950$ with MAPE = 4.01 %, in Fig. 4(g)) and the main peak of SCX ($Q^2 = 0.960$ with MAPE = 4.29 %, in Fig. 4(h)). Obviously, the aggregate predictions of the trained model are lower than the observations, as shown in Fig. 4(b). The DoE runs conducted with high elution pH at a set point +0.3 have smaller deviations, compared to other pH values. The prediction for aggregates has a large systematic offset (MAPE = 33.40 %), and only 56.7 % observations can be well explained by the model ($Q^2 = 0.567$). In Fig. 4(c), almost all the

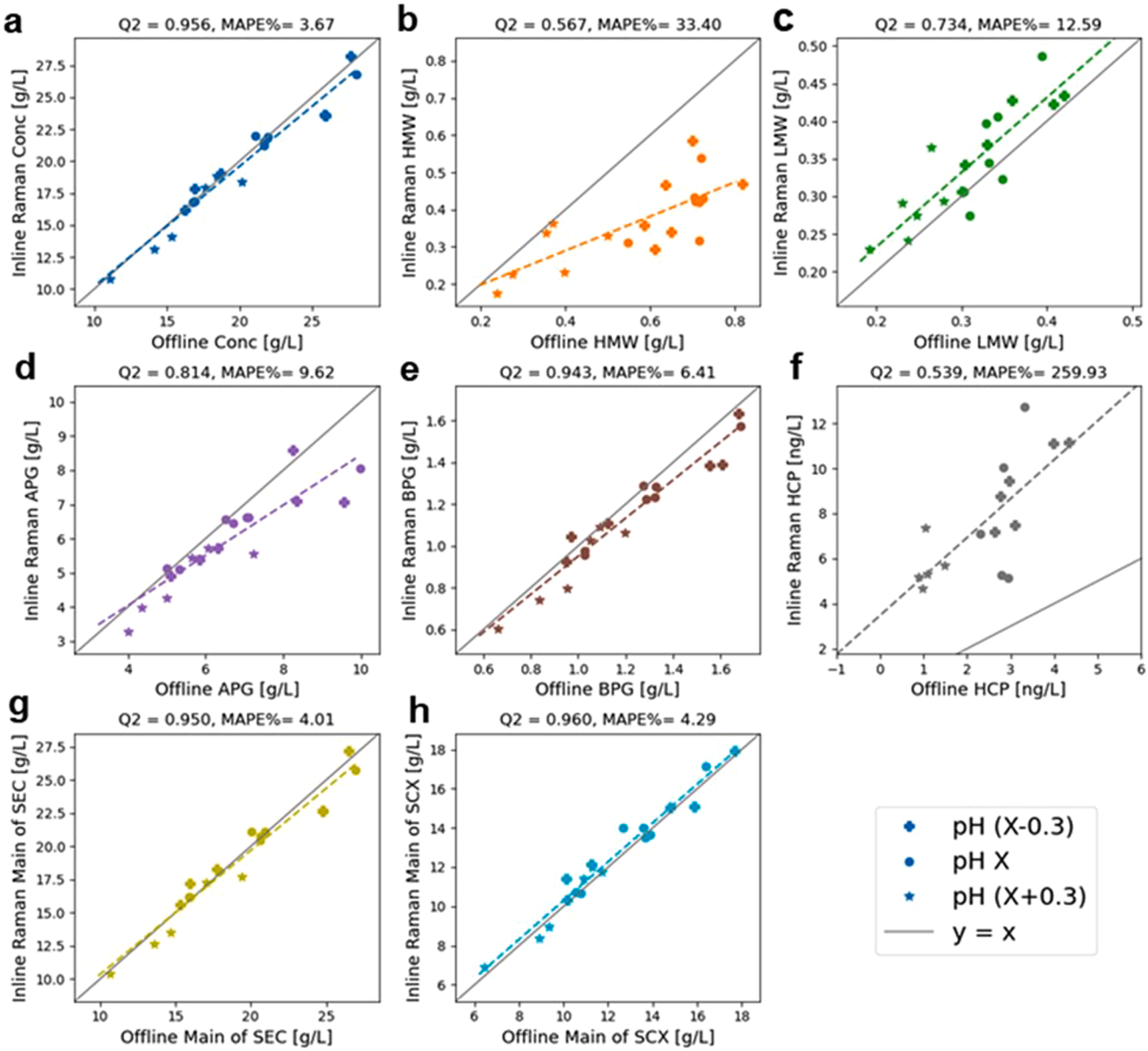

Fig. 4. Comparison between off-line pool analytical measurements and in-line pool predictions derived from in-line Raman profiles for 8 critical quality attributes. The findings were categorized and displayed in a filled plus marker for pH 0.3 smaller than set point, circle marker for pH at set point, and a star marker for pH 0.3 larger than set point. The calibration experiment was performed at pH set point. The corresponding metrics Q2 and MAPE in percent were displayed in the regression plots for (a) protein concentration, (b) high molecular weight (HMW) or aggregates, (c) low molecular weight (LMW) or fragments, (d) acid charge variants APG, (e) basic charge variants BPG, (f) host cell proteins (HCP), the main peak of (g) size variants SEC and (h) charge variants SCX.

predictions on fragments are higher than the observations (MAPE = 12.59 %). The trained Raman model overpredicted HCP concentration with a Q^2 of 0.539 and a MAPE of 259.93 % (Fig. 4(f)).

When comparing the concentration correlations in both Figs. 2 and 4, it appears to be surprising and contrary to the intuition that the model's predictability for the 19 DoE runs shows smaller deviations with significantly lower MAPE values, with the exception of aggregates and HCP. However, the explanation is similarly obvious when considering different approaches of assessing model's prediction accuracy in the internal and external validation were forced to be used. Within the internal validation dataset, as illustrated in Fig. 1, the absolute discrepancy between model's prediction and off-line measurement was evaluated fraction for fraction and finally summed up to the MAPE. As for the DoE runs, however, due to the nature of the non-fractionized analytics, over- and underpredictions within a single DoE run could compensate each other and be hidden in the final overall MAPE, as represented in Fig. 3.

The ANOVA test shows that the elution pH significantly impacts the model's accuracy in predicting aggregates, which aligns with the observed result that experiments with higher elution pH have smaller deviations (Fig. 4(b)). The pH influence can be attributed to the experimental procedure, which involved different sample handling methods during the calibration experiment and the DoE runs. To minimize lab-intensive work, all DoE pool samples were frozen at −70 °C after collection and thawed together for collective SEC and SCX analytics. In contrast, the 26 fractions for model calibration were measured immediately after collection without freeze/thaw treatment. Protein A elution samples under low pH are known to be easily stressed by freeze/thaw treatment, forming more aggregates [25]. Consequently, after freeze/-thaw stress, more aggregates were generated and measured under SEC analytics, resulting in large deviations between predictions and measurements. Except for the pH influence on aggregate prediction, ANOVA test confirms that process parameters have no significant impact on the model's accuracy in predictions, highlighting the model's impressive interpolation ability.

The deviation in fragment prediction originates from the analytical reference methods. Generally, SEC is considered a robust and accurate analytical technique for determination of protein aggregates, whereas underestimation of fragment population [26] in SEC can affect the accuracy of quantifying fragments. One limitation of applying a Raman-based model is that the model calibration is based on the analytical reference methods, thus the model's accuracy will never exceed the reference's accuracy. Capillary electrophoresis with sodium dodecyl sulfate (CE-SDS) is a recommended analytical technique for quantifying the overall fragmentation population [26,27]. Thus, CE-SDS can be an alternative reference technique for the Raman model. Regarding the HCP overpredictions, it is challenging for the Raman model, because the HCP is a lumped CQA consisting of many sub-species. Different process conditions and experimental settings induce the elution of different subsets of HCP in different ratios, resulting in various combinations of Raman spectral features, presenting a major challenge for the data-driven machine learning model to cope with. Broader and more comprehensive subsets of HCP should be considered if a quantitative in-process prediction of HCP is prioritized.

4. Conclusion

In this study, we present a straightforward workflow for generating a PAT tool based on Raman spectroscopy. The underlying model, although trained on a single capture run, is capable of interpolating the profiles of target proteins and impurities in a commercially relevant robustness study with variations in process parameters like loading density, pH, and flow rate. This study signifies the first application of the Raman-based PAT tool for predicting in-line target proteins and seven impurities during Protein A chromatography elution phase at 28-second intervals, conducted in actual DSP scenarios. After validating the Raman-based KNN model with 19 different Protein A chromatography runs, the results confirm the model's robust prediction ability for protein concentration, fragments, charge variants and the main peak of SEC and SCX within an elution pH range of setpoint ± 0.3. These results demonstrate the feasibility of the Raman-based PAT tool to enhance process understanding and promote real-time process monitoring. However, the challenge of limited model predictability at the higher boundary of the pH conditions tested has been revealed. This should be addressed in future investigations. The PAT tool shows potential for quasi real-time decision-making and process optimization based on CQAs during process development, thereby eliminating the need for labor-intensive pooling and sample handling. In addition, the Raman-based tool can also serve as a simplified analytical technique, reducing the analytical burden in applications like high-throughput process development, mechanistic model calibration, or candidate selection with high resolution.

CRediT authorship contribution statement

Jingyi Chen: Writing – review & editing, Writing – original draft, Visualization, Validation, Data curation. **Jiarui Wang:** Methodology, Investigation. **Rudger Hess:** Writing – review & editing. **Gang Wang:** Writing – review & editing, Supervision, Resources, Project administration, Investigation. **Joey Studts:** Writing – review & editing, Resources, Project administration, Investigation. **Matthias Franzreb:** Writing – review & editing, Supervision.

Declaration of competing interest

The authors declare that they have no known competing financial interests or personal relationships that could have appeared to influence the work reported in this paper.

Data availability

The authors do not have permission to share data.

References

[1] S.M. Paul, D.S. Mytelka, C.T. Dunwiddie, C.C. Persinger, B.H. Munos, S. R. Lindborg, A.L. Schacht, How to improve R&D productivity: the pharmaceutical industry's grand challenge, Nat. Rev. Drug Discov. 9 (2010) 203–214, https://doi.org/10.1038/nrd3078.
[2] A.C. Fisher, M.-H. Kamga, C. Agarabi, K. Brorson, S.L. Lee, S. Yoon, The current scientific and regulatory landscape in advancing integrated continuous biopharmaceutical manufacturing, Trends Biotechnol. 37 (2019) 253–267, https://doi.org/10.1016/j.tibtech.2018.08.008.
[3] U. Gottschalk, K. Brorson, A.A. Shukla, The need for innovation in biomanufacturing, Nat. Biotechnol. 30 (2012) 489–492, https://doi.org/10.1038/nbt.2263.
[4] D. Müller, L. Klein, J. Lemke, M. Schulze, T. Kruse, M. Saballus, J. Matuszczyk, M. Kampmann, G. Zijlstra, Process intensification in the biopharma industry: improving efficiency of protein manufacturing processes from development to production scale using synergistic approaches, Chem. Eng. Process. - Process Intensif. 171 (2022) 108727, https://doi.org/10.1016/j.cep.2021.108727.
[5] Food and Drug Administration, Q13 Continuous Manufacturing of Drug Substances and Drug Products, Guidance for Industry. The International Council for Harmonisation (ICH). 2023.
[6] D. Yilmaz, H. Mehdizadeh, D. Navarro, A. Shehzad, M. O'Connor, P. McCormick, Application of Raman spectroscopy in monoclonal antibody producing continuous systems for downstream process intensification, Biotechnol. Prog. 36 (2020) e2947, https://doi.org/10.1002/btpr.2947.
[7] D. Saleh, G. Wang, B. Müller, F. Rischawy, S. Kluters, J. Studts, J. Hubbuch, Straightforward method for calibration of mechanistic cation exchange chromatography models for industrial applications, Biotechnol. Prog 36 (2020) e2984, https://doi.org/10.1002/btpr.2984.
[8] Food and Drug Administration, Guidance for Industry PAT — A Framework for Innovative Pharmaceutical Development, Manufacturing, and Quality Assurance. Pharmaceutical CGMPs. 2004.
[9] M.N.S. Pedro, M.E. Klijn, M.H. Eppink, M. Ottens, Process analytical technique (PAT) miniaturization for monoclonal antibody aggregate detection in continuous downstream processing, J. Chem. Technol. Biotechnol. 97 (2022) 2347–2364, https://doi.org/10.1002/jctb.6920.

[10] Food and Drug Administration, Guidance for industry: Q8(R2) pharmaceutical development. The International Council for Harmonisation (ICH). 2009.
[11] A.S. Rathore, H Winkle, Quality by design for biopharmaceuticals, Nat. Biotechnol. 27 (2009) 26–34, https://doi.org/10.1038/nbt0109-26.
[12] F. Feidl, S. Garbellini, S. Vogg, M. Sokolov, J. Souquet, H. Broly, A. Butté, M. Morbidelli, A new flow cell and chemometric protocol for implementing in-line Raman spectroscopy in chromatography, Biotechnol. Prog. 35 (2019) e2847, https://doi.org/10.1002/btpr.2847.
[13] L. Rolinger, M. Rüdt, J. Hubbuch, A critical review of recent trends, and a future perspective of optical spectroscopy as PAT in biopharmaceutical downstream processing, Anal. Bioanal. Chem. 412 (2020) 2047–2064, https://doi.org/10.1007/s00216-020-02407-z.
[14] L. Rolinger, M. Rüdt, J. Hubbuch, Comparison of UV- and Raman-based monitoring of the Protein A load phase and evaluation of data fusion by PLS models and CNNs, Biotechnol. Bioeng. 118 (2021) 4255–4268, https://doi.org/10.1002/bit.27894.
[15] C.K. Akhgar, J. Ebner, O. Spadiut, A. Schwaighofer, B. Lendl, QCL–IR spectroscopy for in-line monitoring of proteins from preparative ion-exchange chromatography, Anal. Chem. 94 (2022) 5583–5590, https://doi.org/10.1021/acs.analchem.1c05191.
[16] B.A. Patel, A. Gospodarek, M. Larkin, S.A. Kenrick, M.A. Haverick, N. Tugcu, M. A. Brower, D.D. Richardson, Multi-angle light scattering as a process analytical technology measuring real-time molecular weight for downstream process control, mAbs 10 (2018) 945–950, https://doi.org/10.1080/19420862.2018.1505178.
[17] M.B. Taraban, K.T. Briggs, P. Merkel, Y.B. Yu, Flow water proton NMR: in-line process analytical technology for continuous biomanufacturing, Anal. Chem. 91 (2019) 13538–13546, https://doi.org/10.1021/acs.analchem.9b02622.
[18] C. Zhang, J.S. Springall, X. Wang, I. Barman, Rapid, quantitative determination of aggregation and particle formation for antibody drug conjugate therapeutics with label-free Raman spectroscopy, Anal. Chim. Acta 1081 (2019) 138–145, https://doi.org/10.1016/j.aca.2019.07.007.
[19] B. Wei, N. Woon, L. Dai, R. Fish, M. Tai, W. Handagama, A. Yin, J. Sun, A. Maier, D. McDaniel, E. Kadaub, J. Yang, M. Saggu, A. Woys, O. Pester, D. Lambert, A. Pell, Z. Hao, G. Magill, J. Yim, J. Chan, L. Yang, F. Macchi, C. Bell, G. Deperalta, Y. Chen, Multi-attribute Raman spectroscopy (MARS) for monitoring product quality attributes in formulated monoclonal antibody therapeutics, mAbs 14 (2022) 2007564, https://doi.org/10.1080/19420862.2021.2007564.
[20] J. Wang, J. Chen, J. Studts, G. Wang, Automated calibration and in-line measurement of product quality during therapeutic monoclonal antibody purification using Raman spectroscopy, Biotechnol. Bioeng. (2023), https://doi.org/10.1002/bit.28514.
[21] J. Wang, J. Chen, J. Studts, G. Wang, In-line product quality monitoring during biopharmaceutical manufacturing using computational Raman spectroscopy, mAbs 15 (2023) 2220149, https://doi.org/10.1080/19420862.2023.2220149.
[22] T. Williams, K. Kalinka, R. Sanches, G. Blanchard-Emmerson, S. Watts, L. Davies, C. Knevelman, L. McCloskey, P. Jones, K. Mitrophanous, J. Miskin, D. Dikicioglu, Machine learning and metabolic modelling assisted implementation of a novel process analytical technology in cell and gene therapy manufacturing, Sci. Rep. 13 (2023) 834, https://doi.org/10.1038/s41598-023-27998-2.
[23] M.N.S. Pedro, M. Isaksson, J. Gomis-Fons, M.H.M. Eppink, B. Nilsson, M. Ottens, Real-time detection of mAb aggregates in an integrated downstream process, Biotechnol. Bioeng. 120 (2023) 2989–3000, https://doi.org/10.1002/bit.28466.
[24] L. Rolinger, J. Hubbuch, M. Rüdt, Monitoring of ultra- and diafiltration processes by Kalman-filtered Raman measurements, Anal. Bioanal. Chem. 415 (2023) 841–854, https://doi.org/10.1007/s00216-022-04477-7.
[25] L.A. Kueltzo, W. Wang, T. Randolph, J.F. Carpenter, Effects of solution conditions, processing parameters, and container materials on aggregation of a monoclonal antibody during freeze-thawing, J. Pharm. Sci. 97 (2008) 1801–1812, https://doi.org/10.1002/jps.21110.
[26] J. Vlasak, R. Ionescu, Fragmentation of monoclonal antibodies, mAbs 3 (2011) 253–263, https://doi.org/10.4161/mabs.3.3.15608.
[27] O.O. Dada, R. Rao, N. Jones, N. Jaya, O. Salas-Solano, Comparison of SEC and CE-SDS methods for monitoring hinge fragmentation in IgG1 monoclonal antibodies, J. Pharm. Biomed. Anal. 145 (2017) 91–97, https://doi.org/10.1016/j.jpba.2017.06.006.